DUAL-EMITTING Cu-DOPED ZnSe/CdSe NANOCRYSTALS

by

REBECCA SUZANNE SUTTON

B.S. Northwest Missouri State University, 2013

A THESIS

submitted in partial fulfillment of the requirements for the degree

MASTER OF SCIENCE

Department of Chemistry
College of Arts and Science

KANSAS STATE UNIVERSITY
Manhattan, Kansas

2015

Approved by:

Major Professor
Emily McLaurin, Ph.D.

Copyright

REBECCA SUTTON

2015

Abstract

Cu-doped ZnSe/CdSe core/shell nanocrystals were synthesized using the growth doping method. Upon shell growth, the nanocrystals exhibit dual emission. The green luminescence peak is assigned as band edge emission and the broad, lower energy red peak is due to Cu dopant. Although, the oxidation state of Cu in the nanocrystals is debated, the emission is explained as recombination of a hole related to Cu^{2+} with an electron from the conduction band. The emission changed in the presence of dodecanethiol. Generally, the band edge emission intensity decreases and the Cu emission intensity increases. One explanation is the thiol acts as a hole trap, preventing hole transfer to the conduction band. Samples were obtained with varying amounts of Cd^{2+}. In the presence of larger amounts of Cd^{2+}, the nanocrystals had "thicker shells", and both the band edge and Cu emission were less sensitive to thiol. The sensitivity likely decreased because the shelled, larger nanocrystals have fewer surface defects resulting in more available electrons.

Table of Contents

List of Figures

List of Tables

Acknowledgements

The most important people in my life are my family. My parents, Louis and Cathy, have supported me throughout my entire life. My brother, Decker, has been my best friend for many years. No matter the circumstances, he always has my back. Finally, my boyfriend Garrett, no matter the day I had, I could always count on him to make me smile. I also need to thank him for his patience and understanding, and putting up with me. They have all supported me throughout my life and pushed me to be the best I can be. No matter what was happening I could always count on them being there. Through many highs and lows in life they have stood beside me in all I have done. Without their support, patience, and guidance I wouldn't be the person I am today.

I would like to thank my advisor Emily McLaurin for all that she has done for me. I owe her a debt of gratitude for the many hours spent discussing these topics, her guidance, and assistance throughout this project. I would also like to thank my group members Mohammad, Raghavender, Allison, Matthew, Bemnet, and Christi for assisting in research, answering questions, and giving helpful suggestions to further my research. Lastly, I'd like to thank Kansas State University and the Chemistry Department for funding.

Dedication

To my friends and family for their many years of support, guidance, and laughs.

Abbreviations

BE	Band Edge
CB	Conduction Band
$CdOA_2$	Cadmium Oleate
$CdOAc_2$	Cadmium Acetate
CdS	Cadmium Sulfide
CdSe	Cadmium Selenide
Cu	Copper
$CuCl_2$	Copper (II) Chloride
$CuOA_2$	Copper Oleate
$CuOAc_2$	Copper Acetate
$CuSt_2$	Copper (II) Stearate
DDT	Dodecanethiol
EPR	Electron Paramagmetic Resonance
EXAFS	Extended X-ray Absorption Fine Structure
FL	Fluorescence
HDA	Hexadecylamine
IR	Infrared
Mn	Manganese
NC	Nanocrystal
nm	Nanometer
OA	Oleic Acid
ODA	1-octaecylamine
ODE	Octadecene
PL	Photoluminescence
QD	Quantum Dot
QY	Quantum Yield
S	Sulfur
Se	Selenium
SEC	Spectro-electrochemical
TBP	Tri-n-butylphosphine
TMAH	Tetramethylammonium Hydroxide Pentahydrate
TOP	Trioctylphosphine
uL	Microliter
Ut_2	Undecylenic Acid
UV	Ultraviolet
VB	Valence Band
XANES	X-ray Absorption Near Edge Structure

$ZnOA_2$	Zinc Oleate
$ZnOAc_2$	Zinc Acetate
ZnS	Zinc Sulfide
ZnSe	Zinc Selenide
$ZnSt_2$	Zinc Stearate
$ZnUt_2$	Zinc Undecylenate

Chapter 1 - Introduction

Colloidal Semiconductor Nanocrystals

Colloidal semiconductor nanocrystals (NCs) are nanometer-sized crystals made of semiconductor material that combine the chemical and physical properties of molecules with the optoelectronic properties of semiconductors.[1] They can range in size from one nanometer (hundreds of atoms) to one hundred nanometers (more than 100,000 atoms). Not only are they much smaller than bulk semiconductors, but they exhibit different optical properties due to the quantum confinement effects. Figure 1.1 shows the difference in the conduction band (CB) and valence band (VB) for bulk materials, NCs, and molecules.

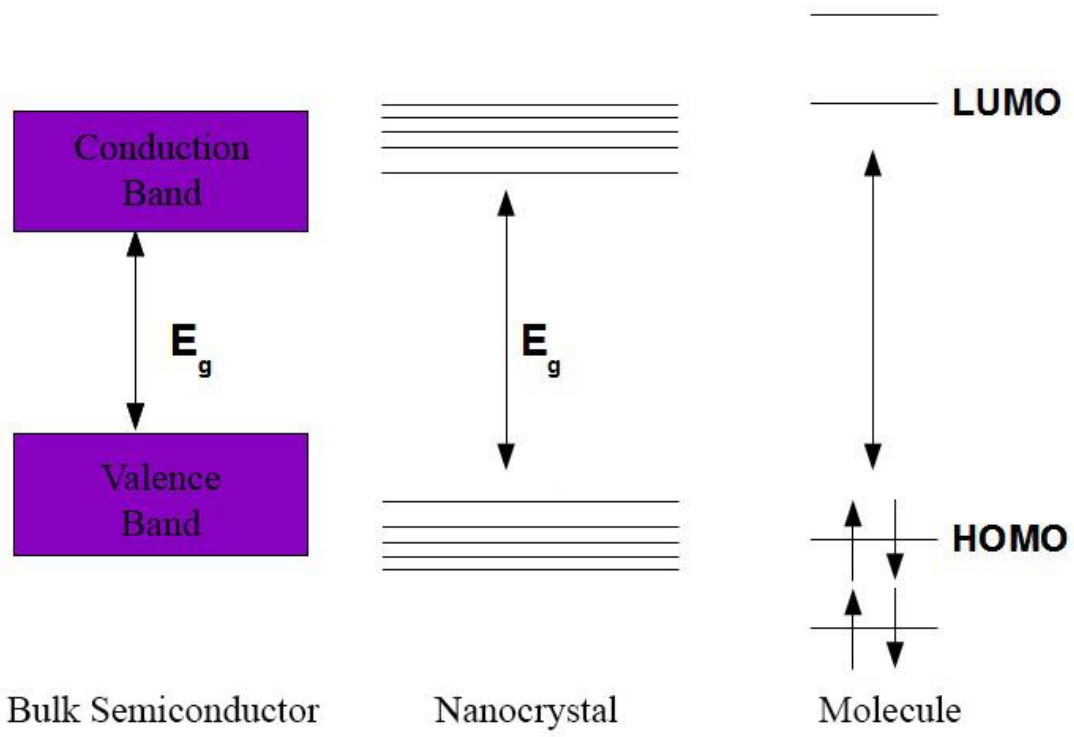

Figure 1.1 Energy levels of bulk semiconductors, NCs, and molecules.

Quantum confinement occurs when the size of the NC is less than twice the Bohr radius of the bulk material. The charge carriers are confined to small regions of space where the dimensions

are less than the de Broglie wavelength.[2] As the size of the particle decreases (to the nanoscale), the decrease in confining dimensions results in discrete energy levels which increases the band gap, and thus the band gap energy. This band gap energy is highly dependent on NC diameter, as seen in Figure 1.2, and plays an important role since size effects determine the absolute energies of the quantum-confined states.[3,4]

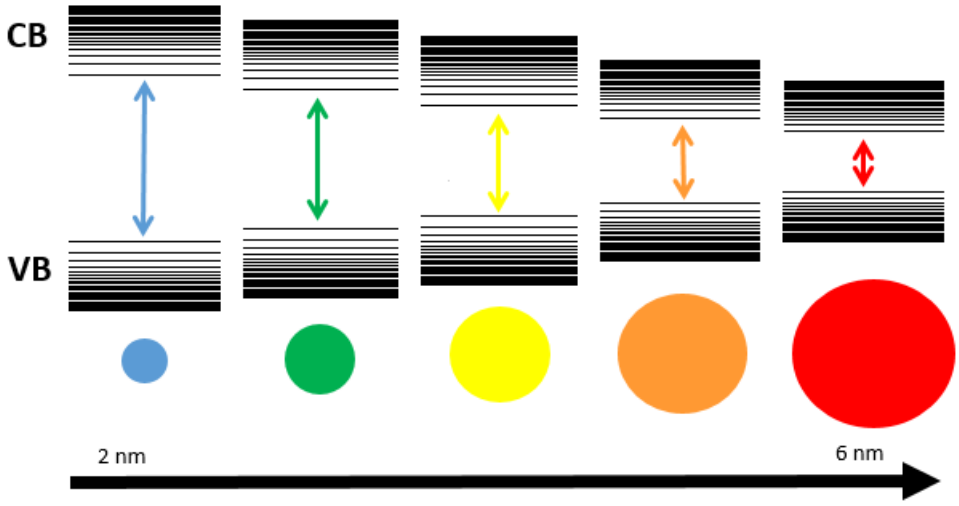

Figure 1.2 Quantum confinement effects on band gap.

The ability to manipulate electrons is important for tailoring the NC electrical and optical properties, leading to a wide array of uses.[5] Colloidal semiconductor NCs have many applications such as light emitting diodes,[6,7] photovoltaic cells,[8] solar cells, sensing,[9,10] and bioimaging.[7] They are popular alternatives to organic dyes due to their large size, broad absorptions, and tunable properties such as absorption and emission, among others.[11] Many of these properties stem from the NC band gap and can be tuned by varying the NC size or composition.

Optical absorption and emission by NCs is similar to that of molecules, with a few key differences. Figure 1.3 shows a diagram of radiative processes in a NC. Upon light absorption (or

electrical excitation), an electron is promoted from the VB to the CB, forming and electron-hole pair (exciton). This absorption is illustrated in Figure 1.3, arrow A. The carriers may radiatively recombine, Process B, resulting in luminescence or non-radiative recombination may occur. Alternatively, the exciton may transfer energy to trap states. Trap states are caused by surface defects, dangling bonds, lattice defects, and impurities. Carriers can relax from trap states non-radiatively or radiatively (Process D). Radiative trap emission is characterized as a broad peak, red-shifted from the BE emission peak. Non-radiative transitions mostly take place on the surface of the NC and can be prevented though passivation of unoccupied surface bonds.[12]

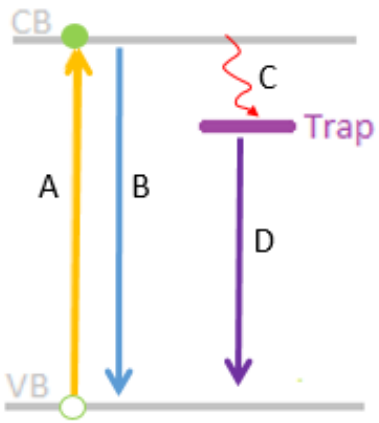

Figure 1.3 Jablonski diagram showing radiative processes that occur in NCs.

Intrinsic Dual-emitting Nanocrystals

Colloidal semiconductor NCs can exhibit two emission peaks when they possess unique electronic structures. The emission is derived from two different excited states within the NCs, one of which is usually ascribed to the excitonic (BE) emission and the other, radiative recombination due to an impurity or trap.[13] A common method for altering NC electronic structure in this fashion is to combine band gap engineering and doping.[9,14] Typically, size is used to tune the band gap energy, but changing composition by introducing a core/shell structure or alloying are alternative methods. The emission can be tuned by changes in the growth conditions[9] and growing a very thick shell can result in different properties such as blinking-free single NC emission, large Stokes shift,[14] and suppressed recombination.[15]

Nanocrystals Exhibiting Trap Emission

As mentioned above, traps are electronic defects that occur in semiconductors, resulting from chemical impurities or an imperfection in the spacing of atoms. They play a significant role in luminescence, photoconduction, and the operation of electronic devices.[16,17] Traps produce intermediate states inside the band gap and can shorten the lifetime of charge carriers by immobilizing a hole or electron preventing its recombination as an electron-hole pair. Thus, BE emission quantum yield usually increases with a decrease in trap states.[17]

Surface properties of NCs play a part in determining their properties, but are poorly understood due to the complexity and variations.[17] The surface is composed of metal cations and anions, many of which are bound to organic ligands.[17,18] These ligands execute multiple functions such as passivating and creating traps, so the concentration and functions of ligands are crucial.[19] For example, as the concentration of trioctylphosphine (TOP) increases in the presence of Cu:ZnSe NCs, the number of surface hole traps decreases, suggesting TOP acts as a hole passivating agent.[19–21]

Impurity Doping

Doping semiconductor NCs with transition metals is of interest because the dopants provide additional tunability, resulting in intense and stable emission in the visible and near-IR region.[7] Although many different transition metals and rare earth metals can be doped into II-VI semiconductor NCs, the doping efficiency varies with synthesis conditions[22] and trends in efficiency are observed with material properties (e.g. valence state and ionic radius).[22] Two popular transition metal dopants for II-VI semiconductor materials are Mn^{2+} and Cu.[23–26] Addition of the dopants generates intermediate energy states between the CB and VB of the host.[17] This changes the NC's photophysical relaxation processes[9,27–29] often resulting in new optical properties

that vary with the composition of the dopants and host.[7] Some properties that make these NCs noteworthy include longer excited-state lifetimes,[28,30] minimized self-absorption,[7,27,31] large emission spectral width,[7,32] and thermal stability.[32] For example, in the case of Mn^{2+}-doped wide bang gap NCs,[27,28] the emission is fixed near 590 nm and Cu-doped NCs have a tunable emission range.[31,32] Mn^{2+}-doped systems have been widely studied, but Cu-doped systems are less well understood. For this reason, the origin of the Cu-dopant emission intensity, tunability, possibility of Cu *d*-states, and emission spectral width are still debated.[7]

Copper Doping

Doping NCs with Cu vs Mn^{2+} has several advantages including a substantially wider tunable emission range[33] (UV to IR), but the NCs are relatively unstable in air.[17] To make Cu-doped NCs viable for applications, stability must be improved,[17] and despite the range of accessible emission energies, they aren't as efficient emitters in II-VI semiconductor hosts as Mn^{2+}. Initially, quantum yields of 2-4% for Cu:ZnSe NCs were reported,[34] with QY of up to 40% reported to-date.[35] One method to achieve higher QY is addition of shells to the doped NCs. These produce higher QY and photostability, both in doped[36,37] and undoped[38,39] structures.

The tunability of Cu-based emission in NCs is related to the surface electronic structure of the host material and concentration of Cu within NCs. Different hosts result in different Cu-emission peak energies and broadness, and the Cu emission often resembles a surface state (trap) emission. This convolution creates doubt in the origin of the emission, specifically whether it involves the Cu or if it is due to a surface trap.[7] The Cu-related emission is due to interaction of the CB with the Cu, and is believed to occur independently of the BE emission.[17,19] Since the Cu *d*-levels do not shift with size, the position of the emission is due to the shift of the CB.[19] The large

spectral width of the Cu emission peak arises from the intrinsic nature of this emission.[40] Cu is known to have $^2T_2$ and ^2E states so the emission is likely a radiative relaxation involving both.[41]

Copper Redox Chemistry

A major issue in understanding the processes involved in the Cu-doped NC emission are the contradicting reports of the Cu oxidation state. Cu^{2+} and Cu^{+} have different electronic structures, d^9 (paramagnetic) and d^{10} (diamagnetic), respectively. Although Cu^{+} salts are sometimes used to synthesize Cu-doped NCs, Cu^{2+} salts are frequently employed as the dopant source. There is some evidence the Cu^{2+} ions retain their +2 oxidation state after being doped into semiconductors.[30,31] In other cases, it is believed that the Cu^{2+} salts are reduced to Cu^{+}.[42,43] Distinguishing between the two states is very important in understanding the optical, magnetic, and electronic properties of these materials.

In Cu:ZnSe/CdSe NCs synthesized with a Cu^{2+} precursor, Klimov and co-workers describe two potential radiative decay pathways based on what form the Cu is in, Cu^{+} or Cu^{2+}. In the case of Cu^{+}, Cu already has a filled orbital (no unpaired electrons), and must capture an external hole before contributing to the emission. On the other hand, Cu^{2+} has an unpaired electron in its $3d^9$ shell, thus it can be considered a state with a permanent optically active hole and participate in emission without injection of a hole.[44] Since they will have different magnetic behaviors based on their electron pairing, the circularly polarized magneto-absorption of the NC was measured in high magnetic fields. The Cu-doped NCs exhibited an enhanced Zeeman splitting, compared to their undoped (nonmagnetic) counterparts. This suggests the Cu dopants are incorporated as the magnetically active Cu^{2+} ions, agreeing with recent EPR studies[30] of Cu^{2+} in ZnSe NCs.[44] They then proceeded to titrate the NCs with dodecanethiol (DDT), a hole-withdrawing species, and observed the changes in luminescence. The undoped NC emission is quenched rapidly by thiol,

but in doped-NCs, a very different situation is present in which there is a gradual growth of the Cu PL peak, with a concomitant decrease in BE PL, resulting in a color change from green to orange. These observations are consistent with the model of Cu in the +2 oxidation state.[44] To look at the effect of varied potentials on the emission spectra and probe the reversibility of the system, Klimov and co-workers used spectro-electrochemcial (SEC) methods. At negative potentials, the Cu peak intensity increases and BE peak decreases in intensity due to the filling of holes. As the potentials become more positive, the exact opposite occurs; the Cu peak decreases with an increase in BE PL. Upon returning back to zero potential, in both situations, the behavior is reversed.[40]

More recently, X-ray spectroscopy was used to examine Cu:CdSe NCs. According to Snee and co-workers, Cu is in the Cu^+ state. XANES was used to characterize the oxidation state of the Cu before and after irradiation. The sample showed a Cu K-edge around 8980 eV supporting the presence of Cu^+, and after the samples were irradiated until no emission was observed (photodarkening), the Cu K-edge shifted to higher energy, indicating oxidation occurred. EXAFS was also performed on the sample before and after photodarkening. After photodarkening, the nearest neighbor scattering amplitude shifted to a longer distance. This means the Cu electrons are mainly scattering off selenium indicating the redox-active Cu ions are translocating within the NC due to oxidation. Oxidation quenches dopant emission and results in an exciton trap state for radiative recombination.[45]

In similar systems, such a Cu:ZnSe and Cu:ZnS NCs, Cu^+ is believed to be present. A Cu^{2+} precursor was used by Pradhan and co-workers, and since the Cu impurities have different electron configurations, electron paramagnetic resonance (EPR) spectra of the NCs will indicate the presence of unpaired electrons present. The Cu^{2+} precursor used showed an EPR signal, indicative of its paramagnetic behavior. The Cu-doped NCs, however, did not have an EPR signal, signifying

Cu^+ is present,[7,42] as they expected from the reduction of Cu^{2+} in the reaction.[7] Although Cu^{2+} is expected to exhibit an EPR signal, the lack of an EPR signal does not confirm the presence of Cu^+.

The variation in luminescence of Cu:ZnSe with photoredox was also examined by Pradhan and co-workers. They irradiated the NCs under UV light in the presence of air, completely quenching the NC emission. Upon adding MPA (or cysteamine hydrochloride, 4-mercaptobenzoic acid, or dodecanethiol), the emission was restored. Thiols are known to act as strong surface binding ligands and BE emission quenchers, but in this case the results suggest they act as surface cleaning agents, removing sulfur to restore emission.[46] After photooxidation, the NCs were reduced using tetrabutylammonium borohydride (Bu_4NBH_4) and emission was restored. The NCs were then re-photooxidized and the emission was quenched once again. Reduction of the NCs using thiols restored the NC emission, and they were stable to photooxidation. This means treatment with borohydride is only temporary, and precipitates the NCs, whereas thiols resist oxidation for a longer period of time.[46] To determine whether the change in emission was due to Cu redox chemistry or photoredox at the surface of the NC, samples were irradiated in air and an inert atmosphere. The samples irradiated in air experienced a rapid (less than one minute) quench of the Cu-dopant emission, but the samples in an inert atmosphere maintained their luminescence for hours. This suggests air is mandatory for photo-darkening, and the emission quench is likely due to surface oxidation.

Ratiometric Sensing

Luminescent NCs have many desirable traits for use as biological sensors such as high quantum yields, photostability, narrow and tunable emission, and broad excitation profiles.[47–49] The long-range goal of this research is noninvasive monitoring of biologically relevant species and physiological parameters.[50] To accomplish this, an ideal sensor would be stable, water-soluble,

non-toxic, and have two emission peaks that exhibit a reversible change in peak intensities in the presence of a specific analyte.[10,51,52] With two peaks present, the ratio of the two can be measured instead of relying on the absolute intensity of one peak.[52] An example of a ratiometric response to an analyte is shown in Figure 1.4. Here, the lower energy peak increases and the higher energy peak decreases and the point where these luminescence curves cross is referred to as the isostilbic point. Monitoring the intensity of the two peaks and isostilbic point provides a robust signal that is not influenced by probe concentration or background.

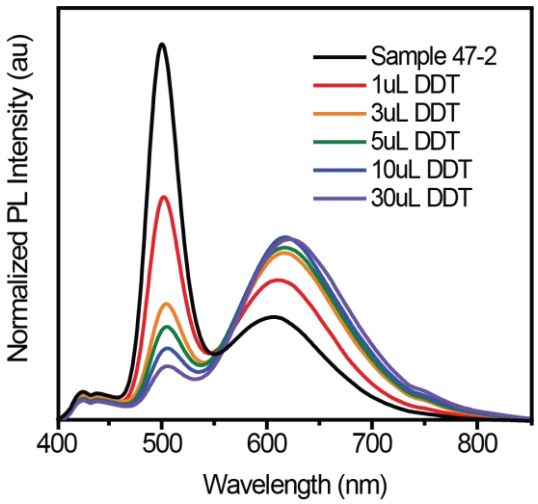

Figure 1.4 NCs with two peaks have dual emission and upon adding an analyte, exhibit a ratiometric relationship.

Of the various types of Cu-doped NCs prepared and redox chemistries explored, only Cu:ZnSe/CdSe NCs exhibited two PL peaks. As described by Klimov, the peaks stem from a reversible Cu^{+}/Cu^{2+} redox couple. We expect the NCs to exhibit dual emission, one peak from the Cu emission and one from the BE recombination, along with a ratiometric relationship upon interaction with dodecanethiol (DDT). The question is, is the system reversible chemically in addition to electrochemically, as Klimov demonstrated. A ratiometric, reversible response to DDT should exist if a Cu^{+}/Cu^{2+} redox couple is present. This reversible redox sensing is valuable for examining biological thiols, such as glutathione, which are important factors in biological processes including cell growth and division and DNA synthesis and repair.[47]

Here, preliminary results exploring the prospect for Cu:ZnSe/CdSe NCs to be used as ratiometric sensors are described. We have taken the Cu:ZnSe/CdSe system, replicated it, and looked at the luminescence response to thiol. A decrease in BE emission peak intensity and

increase in Cu emission peak intensity with addition of thiol suggests the presence of the anticipated Cu^{+}/Cu^{2+} redox response. Exposure to an oxidant will increase the BE emission peak intensity at the expense of the Cu emission peak as Cu goes from +1 to +2. Further thiol addition, should reduce the Cu^{2+} to Cu^{+}, demonstrating reversibility in the luminescent ratiometric response. From there, water-solubility is required for further studies of these NCs as biological sensors.

Chapter 2 - Results, Data, and Methods

Dual-emitting semiconductor NCs have many unique and tunable properties that make them important in a variety of fields. The dual emission we describe comes from two excited states within the same NC: the transition from the conduction band (CB) to the valence band (VB) and CB to impurity level.[22] Adding an impurity dopant introduces a new energy level within the band gap and decreases the NC's sensitivity to thermal, chemical, and photochemical disturbances. Using Cu as a dopant results in better tunability of NC emission, but poor quantum yields. Introducing a shell creates NCs with higher QY and increased stability.

Cu-doped ZnSe/CdSe

Cu-doped ZnSe/CdSe core/shell NCs can exhibit dual emission. One emission peak is believed to come from the Cu and one from the NC. These NCs were first synthesized by Klimov and co-workers[44] using a shell growth method. As shown in Figure 2.1, Cu:ZnSe/CdSe NCs are synthesized using a well-established hot injection method. The ZnSe cores were first synthesized from $ZnSt_2$ and TBPSe. To the cores, $CuOA_2$ was added, then $ZnUt_2$. After the $ZnUt_2$ layer formed, a CdSe shell was grown with $CdOA_2$. Following Cd^{2+} addition, dual emission is observed. Figure 2.2 shows a PL spectrum of a sample at room temperature in toluene. The peak near 600 nm is ascribed to Cu impurities and the higher energy peak is based on band edge (BE) emission.

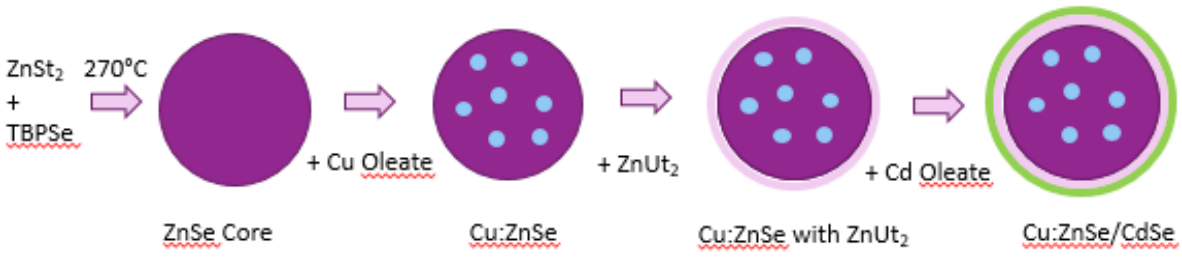

Figure 2.1 Reaction scheme of Cu:ZnSe/CdSe

The peak assignment is explained in terms of Cu oxidation state by Klimov and co-workers. Cu^{+} has filled *d*-orbitals and cannot contribute to the emission without first capturing an external hole. Cu^{2+} has an unpaired electron and can contribute without capturing a hole. It is shown in Figure 2.3a that Cu^{+} first captures a hole from the VB, then the electron from the CB recombines with the Cu hole to produce emission. In the case of Cu^{2+}, Figure 2.3b, Cu already has an unpaired electron and can capture an electron from the CB to participate in the recombination process.

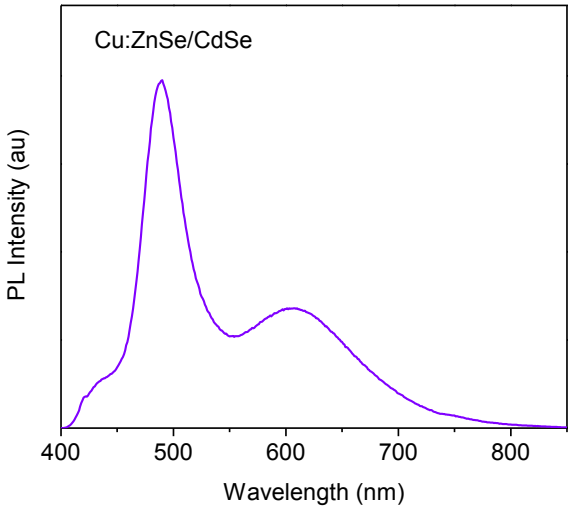

Figure 2.2 Dual emission of a Cu:ZnSe/CdSe NC. The peak near 500 nm is due to the BE and the peak near 600 nm is from Cu impurities.

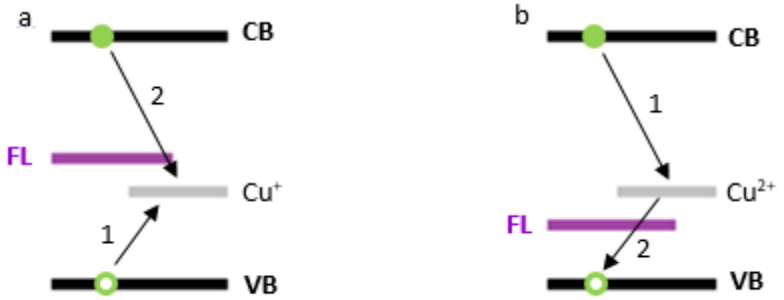

Figure 2.3 Recombination processes of (a) Cu^{+} and (b) Cu^{2+}. (a) Cu^{+} must capture an external hole from the VB, then an electron from the CB recombines with the hole. (b) Cu^{2+} has an unfilled shell (a hole) and captures an electron from the CB to participate in the recombination process.

For a sample synthesized using the method from Figure 2.1, aliquots were taken during growth and dual emission was observed. Figure 2.4 shows the absorption and PL of the aliquots during growth. It is shown that as the NCs get larger, the absorption and emission red shift. Two peaks are observed in the emission spectra of the NCs during shell growth. Although both peaks red-shift, differing peak ratios are observed. Overall, the BE emission peak decreases with-respect-to the Cu peak.

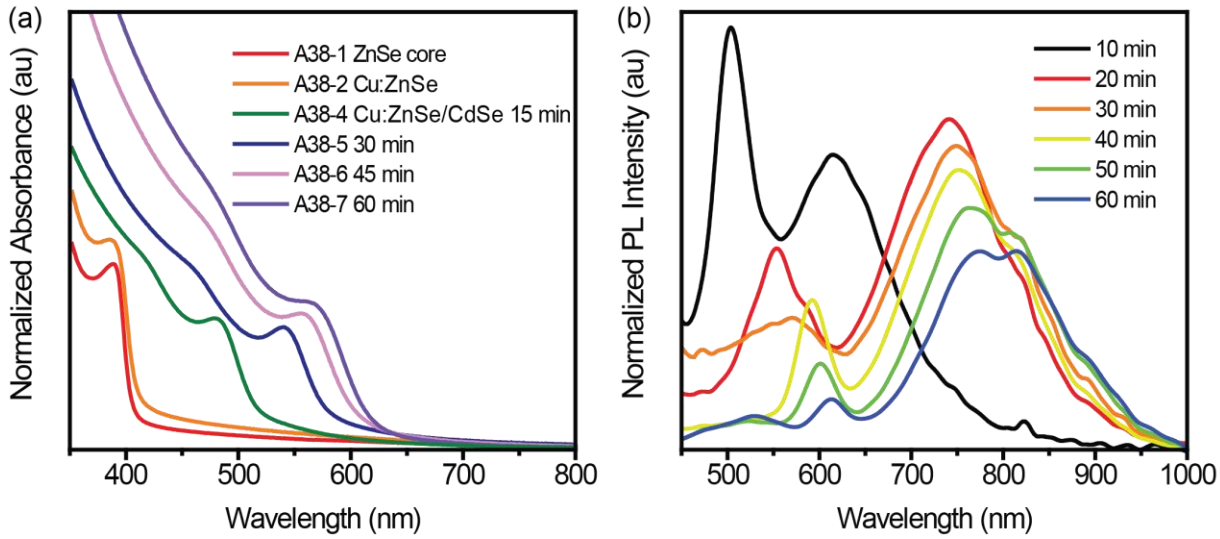

Figure 2.4 Absorption and PL of Cu:ZnSe/CdSe NC growth. With increasing size, the absorption and emission is red shifted.

The absorption and emission of a Cu-doped ZnSe/CdSe NC sample synthesized using the method described above are shown in Figure 2.5. The absorption peak near 490 nm is characteristic of the NC first excitonic feature. The emission peak at 500 nm is ascribed to the BE emission and the peak at 610 nm is due to the Cu impurity. To this sample, dodecanethiol (DDT) was added. Thiol addition was shown to increase the Cu emission with a concomitant decrease in band-edge emission. The current interpretation of this ratiometric luminescence behavior from the literature was explained previously by reduction of the Cu center with thiol, from Cu^{2+} to Cu^{+}, since thiol acts as electron-donating (hole-withdrawing) species.[44] Added electrons fill VB holes allowing the Cu electrons to freely

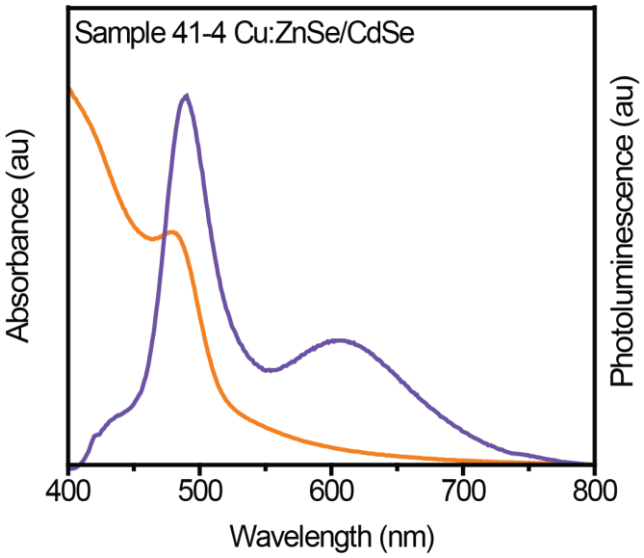

Figure 2.5 Absorption and emission spectra of dual-emitting Cu:ZnSe/CdSe NCs. The peak near 490 nm is characteristic of the NC. The emission peak at 500 nm is ascribed to the BE emission and the peak at 610 nm is due to the Cu impurity.

participate in the recombination process, Figure 2.3. Upon thiol addition, the VB hole is filled, preventing BE electron-hole recombination. Instead, the emission results from recombination of the Cu-hole and a CB electron, as shown in Figure 2.3a.

DDT alone drastically changed NC PL, so a dilute solution (10 uL DDT in 400 uL toluene, 0.0104 M) was used for titrations. To a sample of NCs in toluene, the DDT solution was added in 1 uL increments. After stirring for 30 s, a PL scan was taken using 380 nm excitation. Figure 2.6a shows the emission of Cu-doped ZnSe/CdSe with increasing amounts of DDT. An increase in Cu PL and a decrease in BE PL is observed. Spectra exhibiting this behavior were normalized to total integrated emission intensity. If a hole is present for a long period of time, recombination is primarily due to the band-to-band transition, and results in an emission dominated by BE emission. If a hole is quickly removed (such as when DDT is added), the recombination is primarily due to band-to-Cu transition and is dominated by the Cu emission.[44] Figure 2.6b shows a picture of the visual change in PL. The left vial shows a green emission from the original sample (dominated by BE emission), and the vial on the right shows the emission after DDT is added and the emission is primarily from Cu.

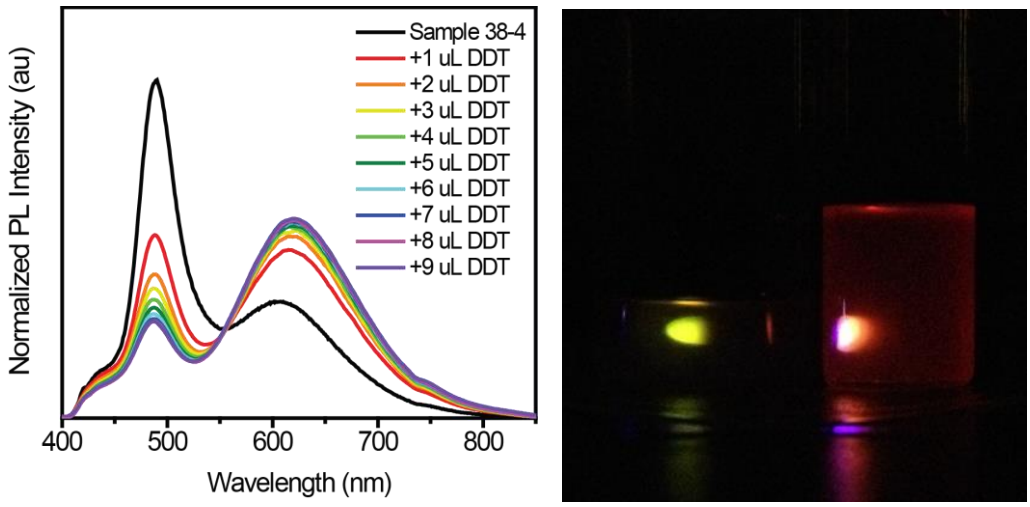

Figure 2.6 (a) PL spectra of Cu:ZnSe/CdSe upon DDT addition and (b) Visual change in emission of sample before (left) and after (right) DDT was added. It is shown that upon DDT addition, the BE decreases and the Cu impurity peak increases.

To quantify the response of BE and Cu PL, the PL intensities were plotted vs. µmoles DDT added. After the first addition, the Cu peak increased and the BE peak decreased in intensities. This trend continued until 0.1 µmoles of DDT were added and then there is little change in the NC PL. The plot in Figure 2.7 shows the changes and saturation point of the NC PL peaks.

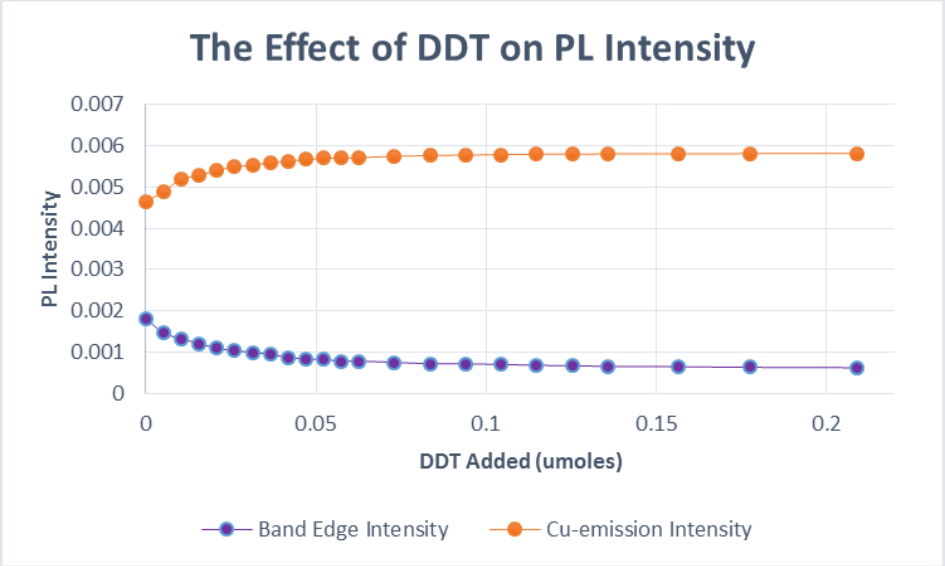

Figure 2.7 S-plot of how DDT effects PL. Upon adding more DDT, a concomitant shift in peak intensities is observed.

Different CdSe shell thicknesses were grown to study the sensitivity of the NCs to DDT and see if there was a change in the response. The shell thickness refers to the amount of $CdOA_2$ added, actual shell thickness were not confirmed. The absorption and emission of these samples are shown in Figure 2.9. After the first addition of DDT solution, the thin shell sample showed the expected PL change. Upon subsequent additions, the Cu peak decreased and the BE peak increased. This is shown in Figure 2.8a. Shells of medium thickness, shown in Figure 2.8b, and thick shells, shown in Figure 2.8c, exhibit the concomitant shift of Cu increasing in intensity and BE decreasing as expected.

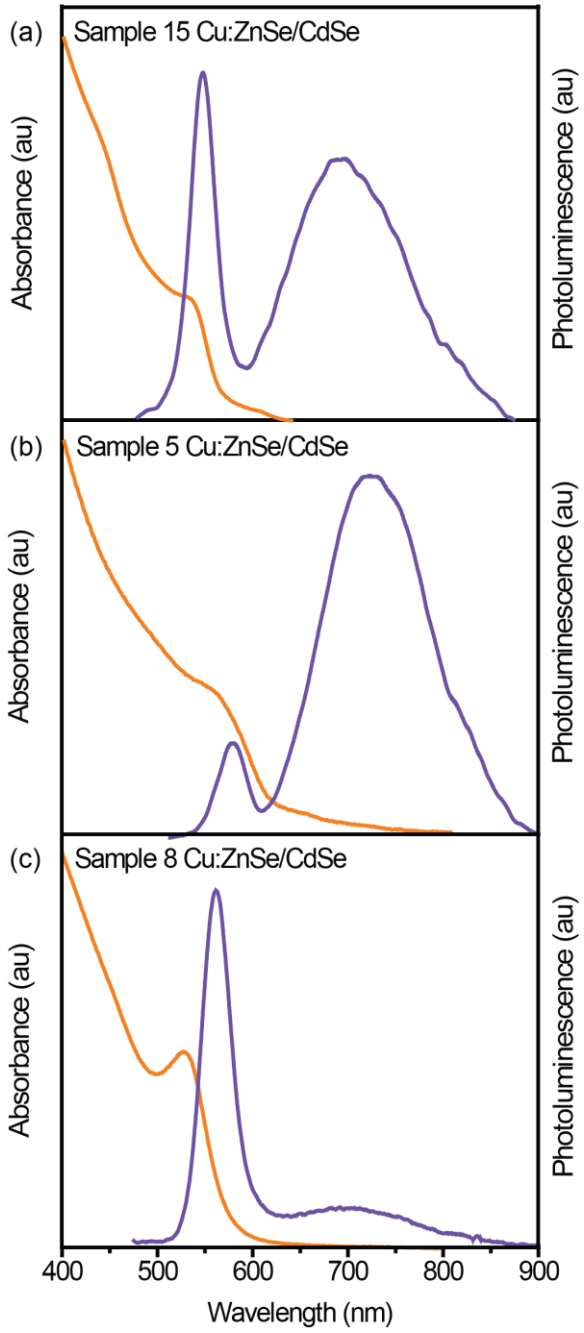

Figure 2.9 Absorption and emission of samples with different shell thicknesses; (a) Thin shell (0.5 ml $CdOA_2$ added), (b) medium shell (1.0 ml $CdOA_2$ added), and (c) thick shell sample (3.0 ml $CdOA_2$ added).

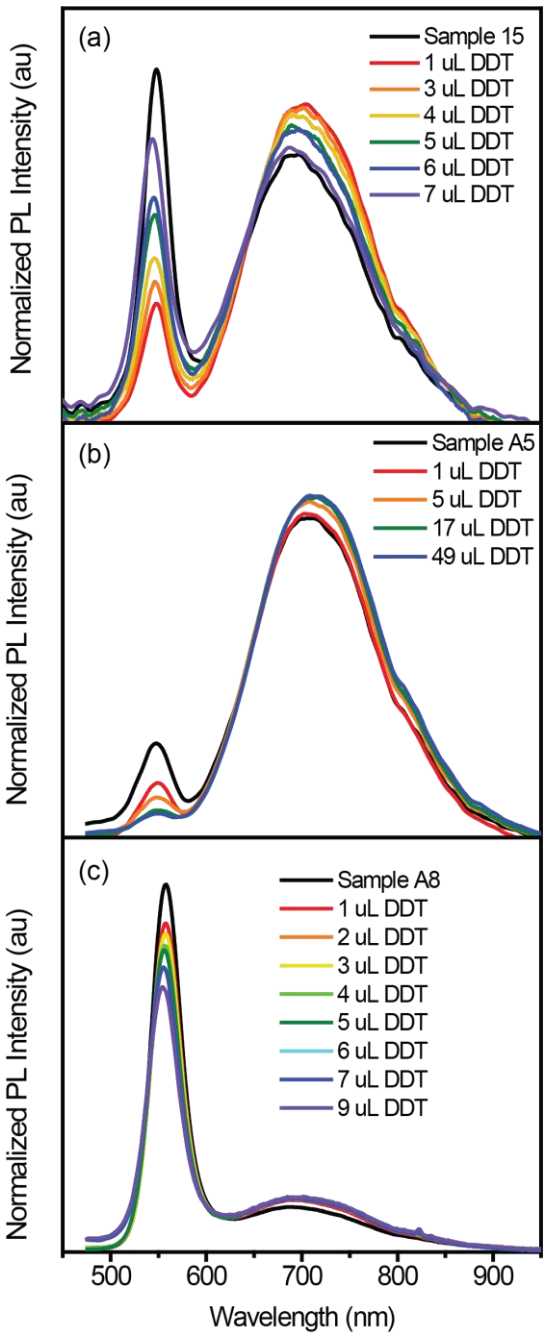

Figure 2.8 PL of different shell thicknesses upon addition of DDT. (a) Thin shell samples shows expected shift upon the first addition, then reversed with subsequent additions of DDT. (b) and (c) Medium and thick shell samples (respectively) exhibit the expected concomitant shift

Although these samples had intentional synthetic variations in shell thickness, generally control of NC photophysical properties was limited. For example, Figure 2.10a shows a sample

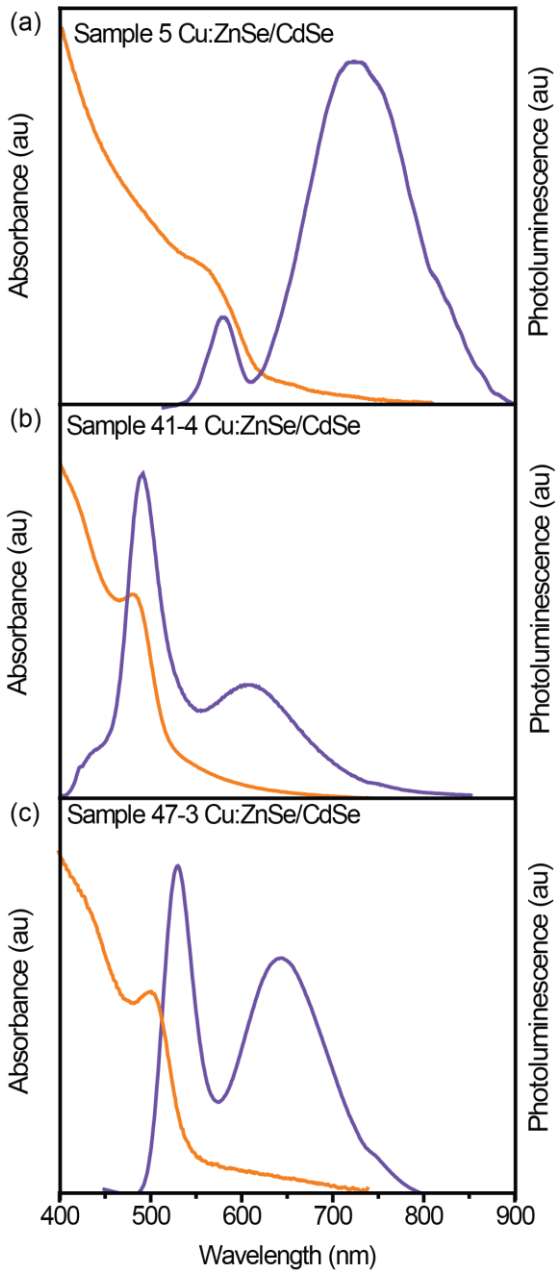

Figure 2.10 Absorption and emission of different Cu:ZnSe/CdSe samples. Variations in synthetic conditions can cause the intensity of BE and Cu emission to vary.

with 525 nm absorption and a high intensity Cu-emission, while a sample with small unintentional variations in synthesis exhibits very different PL (Figure 2.10b and c); sometimes the Cu-based PL is more intense and sometimes the band-edge is more intense. Variations, exacerbated by the multiple step synthesis, may be due to the degassing length, temperature, core size, shell size, number of particles, and amount of copper in NC. Response of the NCs to the addition of DDT also varied from sample-to-sample. Figure 2.11 shows the thiol response in several samples. Samples shown in Figure 2.11a, c, d, f, g, and h exhibited the expected concominant behavior as previously described, the BE peak decreases and Cu impurity peak increases. Even though some samples saw a large change in the Cu emission, others saw very little. In some cases, there is no change in the BE emission. Other samples exhibited different changes in PL peak intensities. Figure 2.8a shows an increase in Cu-emission, but after adding 3 uL DDT, the PL decreases. In Figure 2.11e, both peaks decreased in response to thiol. In Figure 2.11b, the BE peak decreased while the Cu peak remains constant. In some cases (Figure 2.11b, c, and f) an extra peak appears at higher energy, this could be caused

by ligands or undoped NCs since ZnSe emits in this region. In other samples, there is a peak that appears in between the Cu and BE peak that could be from undoped NCs (Figure 2.11d). The shoulder around 750 nm (Figure 2.11f and h) is ascribed to surface traps.[53]

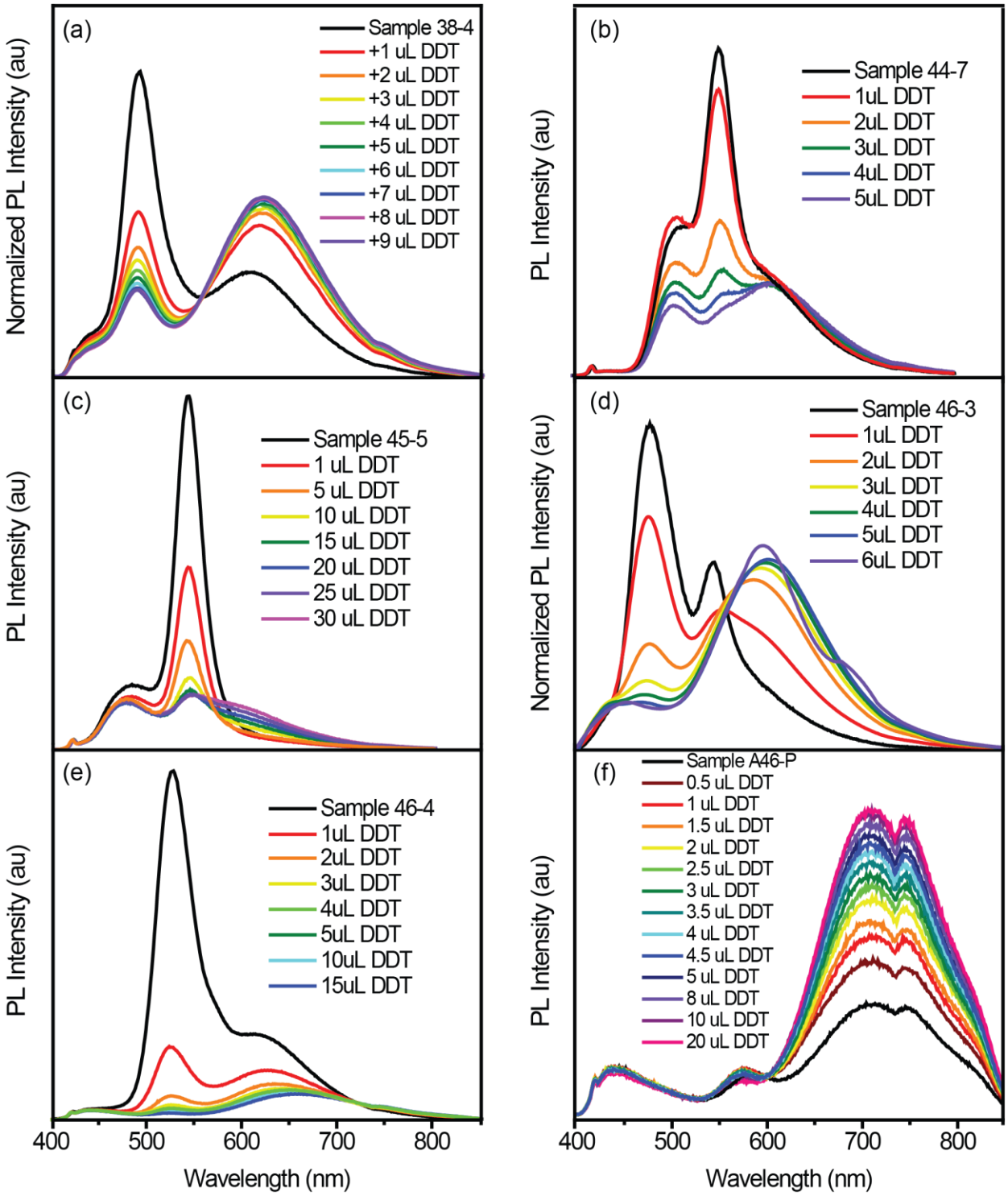

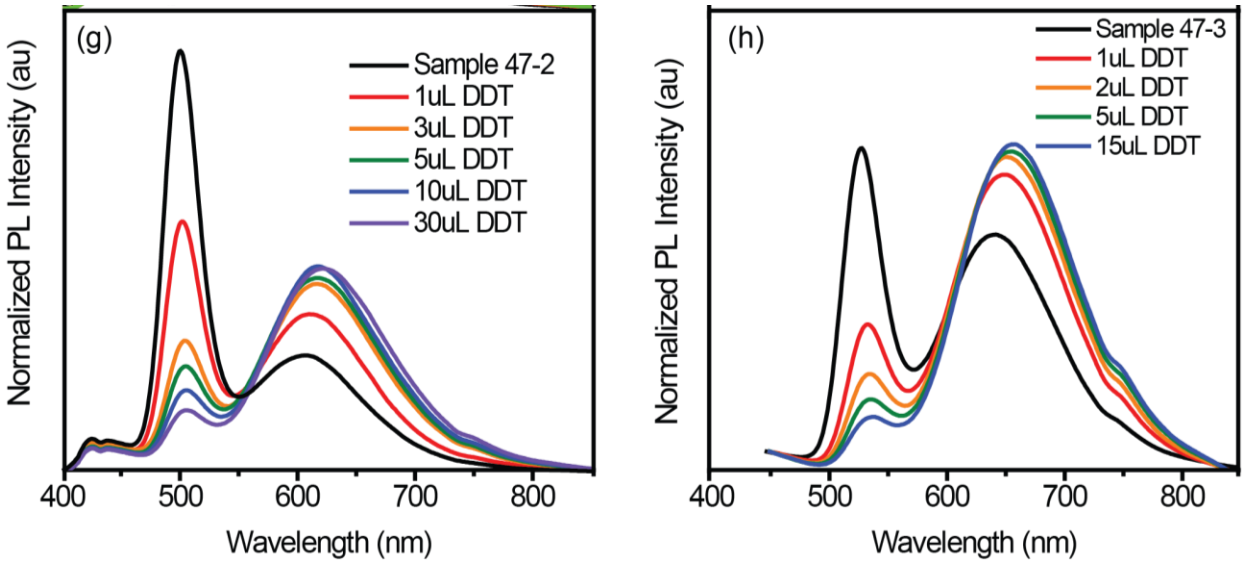

Figure 2.11 PL response of the NC to thiol. Different samples exhibit different responses, but in all of these cases, the BE peak decreases and the Cu peak increases.

A summary of the Cu and BE emission with corresponding procedural differences for samples shown in Figure 2.10 and Figure 2.11 are summarized in Table 2.1. ΔE corresponds to the energy difference between the maximum of the Cu and BE peaks. For a given reaction, such as A38, samples with longer Cd^{2+}-shell growth times exhibited a red-shift in excitonic and Cu luminescence peaks. Sample A46-3 has the highest energy BE and Cu peaks. This sample was synthesized with Cu and $ZnUt_2$ injection temperatures of 190 °C, then decreased to 120 °C for 48 hours, and then Cd shell was grown for 15 minutes. Sample A24-13 has the lowest energy BE and Cu peaks. It was synthesized with a Cu injection temperature of 180 °C, $ZnUt_2$ injection temperature of 190 °C then decreased to 120 °C for 48 hours, and the Cd was injected at 180 °C over 1 hour for shell growth. Sample A44-7 has the smallest energy difference between BE and Cu peaks. It was synthesized with Cu and $ZnUt_2$ injection temperatures of 180 °C, after $ZnUt_2$ injection temperature was decreased to 120 °C for 48 hours, and the Cd was injected at 180 °C for 15 minutes then decreased to 120 °C for 3 hours. The highest energy difference was in Sample A24-9. It was synthesized with a Cu injection temperature of 180 °C, $ZnUt_2$ injection temperature

of 190 °C then decreased to 120 °C for 48 hours, and the Cd was injected at 180 °C over 22 minutes for shell growth.

Table 2.1 Peak intensities and experimental details of samples shown in Figure 2.9 and 2.11.

Sample	BE Peak		Cu Peak		ΔE (eV)	Rxn temp of Cu injection (°C)	Rxn temp of $ZnUt_2$ injection (°C)	Time of shell growth
	nm	eV	nm	eV				
A38-4[a,b]	495	2.51	615	2.02	0.49	150	160	15 m
A38-5[a,b]	571	2.17	695	1.78	0.39			30 m
A38-7[a,b]	591	2.10	723	1.72	0.38			60 m
A38-8[a,b]	595	2.08	725	1.71	0.37			75 m
A24-8[b,c]	503	2.47	615	2.02	0.45	180	190	10 m
A24-9[b,c]	550	2.25	735	1.69	0.57			22 m
A24-11[b,c]	593	2.09	752	1.65	0.44			40 m
A24-13[b,c]	613	2.02	773	1.60	0.42			60 m
A48-6[a,b]	519	2.39	628	1.97	0.41	190	none	22 m
A46-3[b,c]	479	2.59	547	2.27	0.32		190	15 m
A47-2[b,c,d]	499	2.48	605	2.05	0.44			12 m
A47-3[b,c,d]	530	2.34	644	1.93	0.41			20 m
A15[e,f,g]	548	2.26	693	1.79	0.47			24 h
A44-7[b,c,h]	549	2.26	624	1.99	0.27			15 m
A8[i,j,k]	557	2.23	692	1.79	0.43			24 h
A46-9[b,c]	576	2.15	692	1.79	0.36			65 m
A5[g,k,l]	548	2.26	709	1.75	0.51		210	48 h

a) After Cu oleate injection, maintained for 45 min, then the temperature was decreased to 120 °C overnight; b) Cd oleate was injected at 180 °C and aliquots were taken; c) After addition of $ZnUt_2$, the temperature was decreased to 120 °C for 48 hours; d) After Cu oleate injection, temperature was decreased to 120 °C for 48 hours; e) After Cu oleate injection, maintained for 2 hours; f) 0.5 mL of Cd oleate was injected; g) Cd oleate was injected at 210 °C, temperature was decreased to 120 °C overnight; h) After Cu oleate injection, maintained for 15 minutes, then decreased to 120 °C for 3 hours; i) After Cu oleate injection, maintained for 30 min; j) 3.0 mL of Cd oleate was injected; k) Cd oleate was injected overnight at 120 °C; l) 1.0 mL of Cd oleate was injected.

To more closely examine the possible redox processes, samples were oxidized using air. Slow evaporation of toluene over 48 hours was followed by resuspension. It is believed that oxidizing the sample quenches the Cu emission, since electrons are lost. Upon reducing the Cu with DDT, the emission

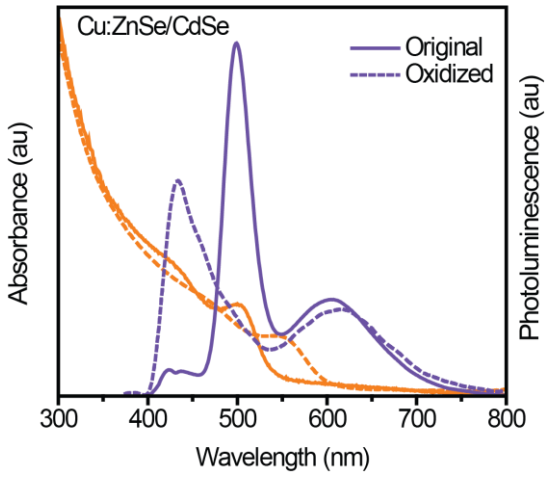

Figure 2.12 Absorption and PL of original sample (solid line) and oxidized sample (dotted line).

should return. After exposing the sample to air for 48 hours, the emission intensity of both peaks decreased (Figure 2.12). There is a change in peak position of the higher energy peak and after comparing the absorption and PL spectra (Figure 2.12), it is shown that the peak near 440 nm is not from the NC. It is likely that oxidizing the sample completely quenched the BE emission and the peak that is observed is from ligands/undoped NCs. When thiol was added, the Cu emission increased past the intensity of the initial (unoxidized) sample, as expected. Figure 2.13 shows the PL of the oxidized sample and the DDT-reduced sample. To see if the reaction was reversible, the sample was dried in air again. Upon adding DDT, the Cu emission increased in intensity and the peak at higher energy decreased (Figure 2.14).

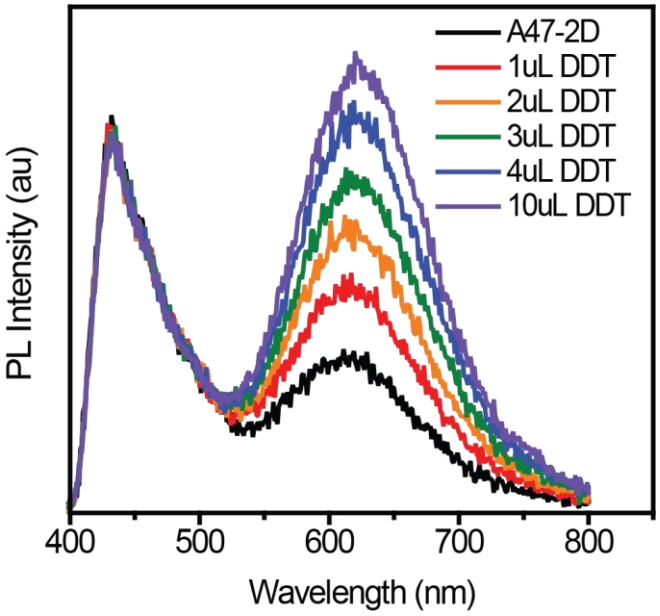

Figure 2.13 PL of a sample being reduced with DDT after it was oxidized. The NCs still exhibit the concomitant shift, although the BE peak has blue shifted ~75 nm.

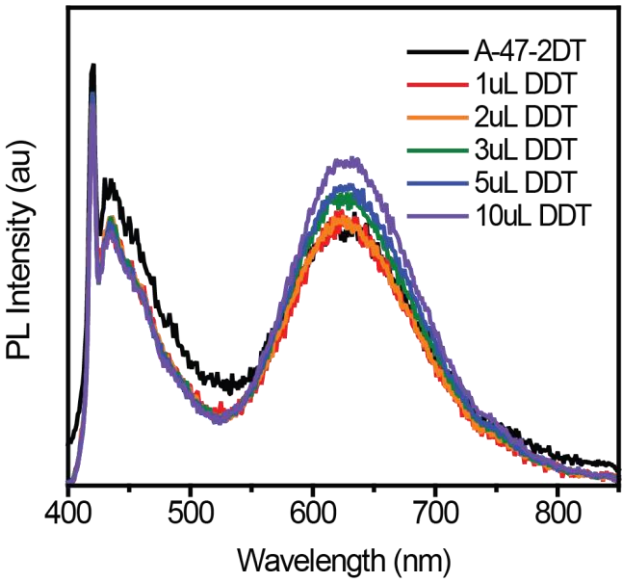

Figure 2.14 PL of a sample being reduced with DDT after it was oxidized, reduced, and then oxidized. The concomitant shift still exists, although the changes are smaller than previously.

To look at the temperature sensitivity of the PL, Cu:ZnSe/CdSe NCs were cooled in liquid nitrogen and the emission was monitored as the samples warmed up (Figure 2.15) As expected, both peaks increased with temperature decrease.[54] In addition, a blue-shift in both the BE and Cu peaks is observed as temperature decreases.[55]

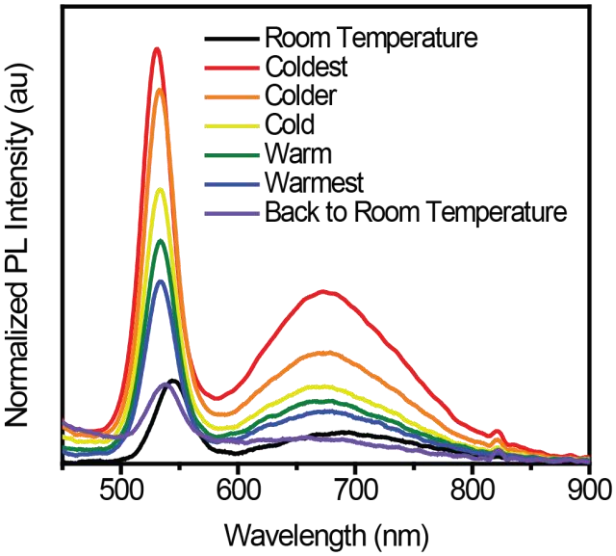

Figure 2.15 PL of sample cooled with liquid nitrogen. The intensity increases as temperature decreases.

Undoped ZnSe/CdSe

There are many examples in the literature of Cu-doped NCs with two PL peaks, where the higher energy peak is attributed to undoped NCs. To investigate the cause of the higher energy emission peak in these samples, a control sample was prepared without Cu. Figure 2.16 shows the absorption and emission spectra of this sample. Aliquots were taken during CdSe addition and a red-shift in absorption and emission spectra were observed (Figure 2.17). Only one PL peak was observed, indicating that one peak, not two, comes from the NC.

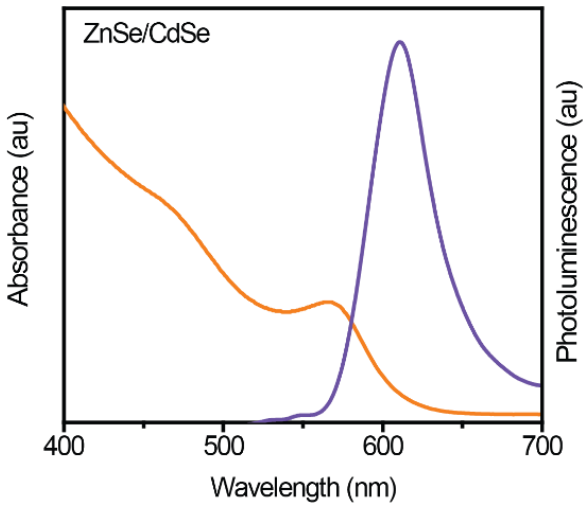

Figure 2.16 Absorption and PL of ZnSe/CdSe NCs. There is an absorption peak at 575 nm and one emission peak at 610 nm due to the BE emission

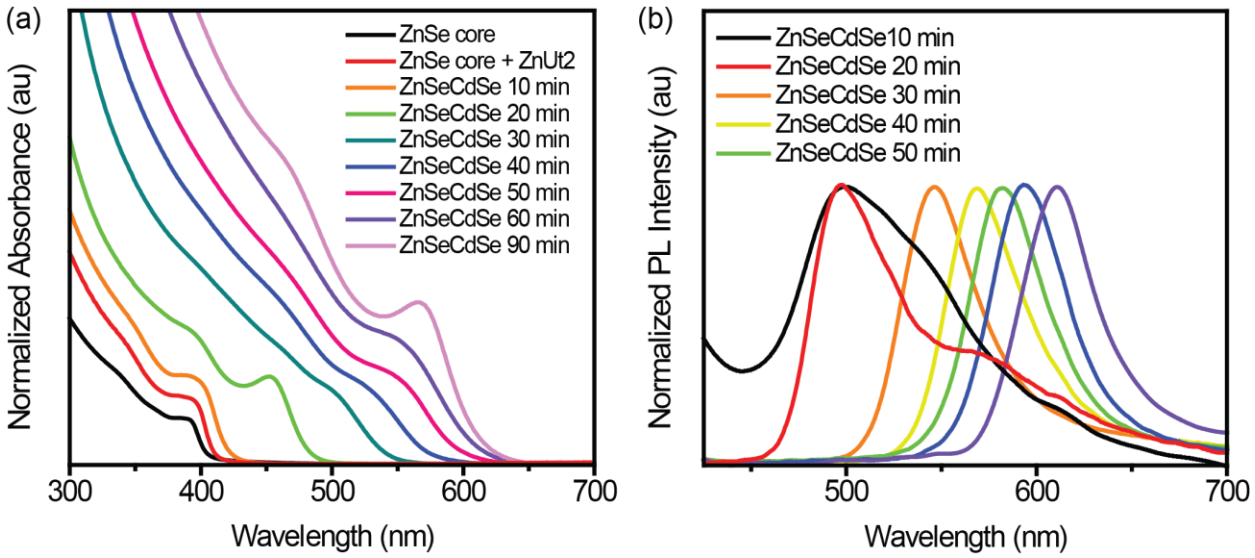

Figure 2.17 Absorption (a) and PL (b) of CdSe shell growth shows the size increasing with a red shift in absorption and emission.

Cu-doped ZnSe

To examine the impact of Cu further, samples without the CdSe shell were synthesized. The absorption of these Cu:ZnSe NCs are shown in Figure 2.18. The first excitonic absorption is at 400 nm. These NCs are brown in color by eye, which can be seen in the tail of the absorption, this color is possibly due to CuSe.[35]

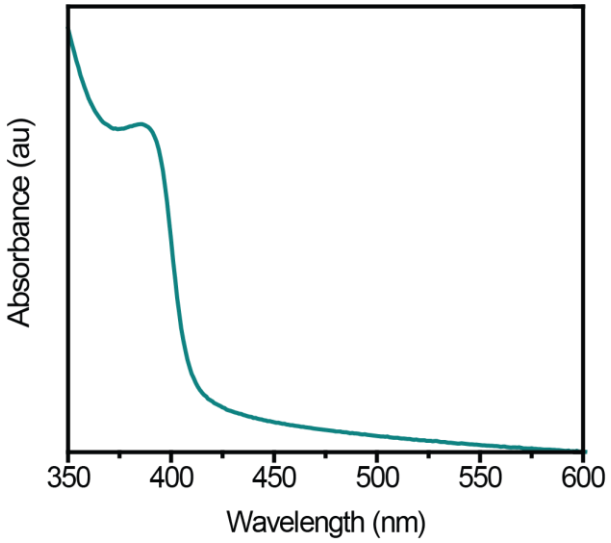

Figure 2.18 Absorption and PL of Cu:ZnSe. Emission peak near 425 nm is characteristic of ZnSe NCs.

Cu-doped ZnSe/ZnSe

To address the effect of Cd oleate addition, Zn oleate was added instead. Figure 2.19 shows the absorption and emission of these NCs. In comparison to those with a CdSe shell, there is only one emission peak observed and it is in the area a ZnSe peak would appear. Without adding a CdSe shell, no Cu emission is observed. The shell material alters the NC emission, as expected, due to the large difference in band gap energy (1.7 eV for CdSe and 2.7 eV for ZnSe). This indicates that no "shell" actually formed and that coating the NC with the same material for a shell as that in the core doesn't create a core/shell structure, but more of an internally doped NC. So the NC should exhibit the same properties as Cu:ZnSe, and is simply a doped NC. It is also possible that upon adding Zn oleate, the Cu leached out of the system and it was no longer doped or a core/shell structure may not be required for dual emission, but rather it presents the required electron structure or conditions needed to observe the Cu emission.

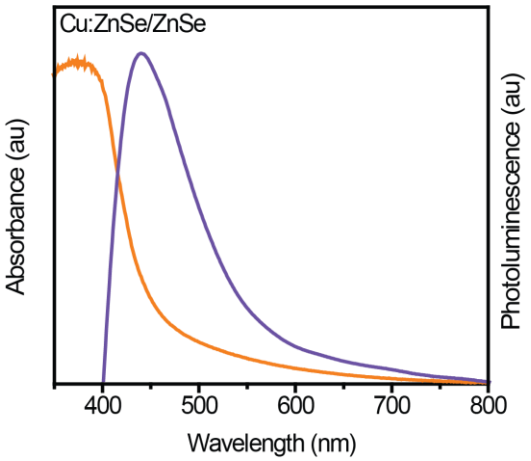

Figure 2.19 Absorption and PL of Cu:ZnSe/ZnSe NCs. The emission peak is characteristic of Cu:ZnSe emission.

No $ZnUt_2$

Finally, step 3, the addition of $ZnUt_2$, was omitted. No differences in the absorption and PL were observed, as shown in Figure 2.20. Despite this, other reasons for the $ZnUt_2$ that are not readily apparent may exist, like filling Zn^{2+} lattice defects in the ZnSe core, or removing hole traps.

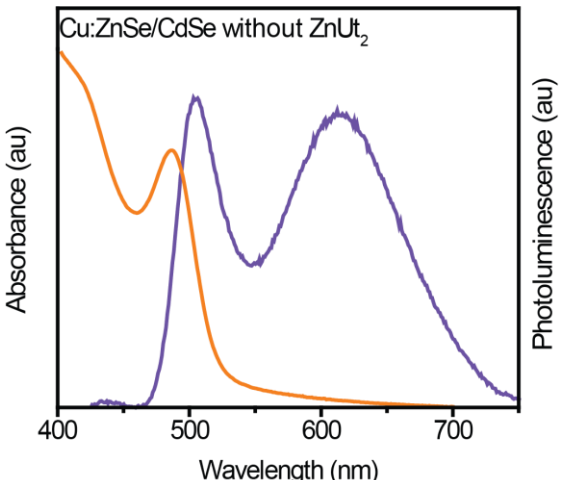

Figure 2.20 Absorption and PL of Cu:ZnSe/CdSe without $ZnUt_2$. The spectra is the same as when $ZnUt_2$ is added.

Discussion

To help explain the effect of DDT on the NC PL, Figure 2.21 shows a possible electronic interaction of DDT with the NC CB, VB, and Cu-state (a) and the structure of DDT (b). DDT is an electron donating, or hole withdrawing species in which the lone pairs on sulfur can act as hole traps. Thiols donate one lone pair to the Cu and the others serve as traps for the VB holes.[56]

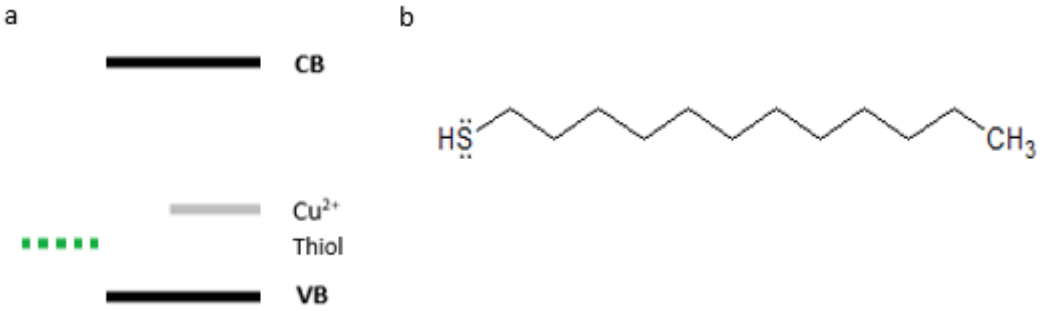

Figure 2.21 (a) Proposed electronic structure of Cu-doped ZnSe/CdSe with thiol and (b) Structure of dodecanethiol (DDT)

In the presence of Cu, Klimov describes the effect of thiol on Cu-doped NCs as a change in oxidation state, from Cu^{2+} to Cu^{+}. Figure 2.3 shows the recombination processes. In the Cu^{2+} state, Cu already has one unpaired electron, which can capture an electron from the CB resulting in recombination. Figure 2.21a shows the electronic structure of the NC in which the thiol energy level resides between the Cu level and VB. Since the Cu^{2+} is closer to the thiol than the CB, the Cu will capture electrons from the thiol instead of those of the CB, producing a Cu^{+} emission. This assumes the thiol only interacts with the Cu, as mentioned above, and the Cu^{2+} is reduced to Cu^{+}.

An alternative explanation considers multiple types of interactions between the thiol and NC. Figure 2.21 can help explain interactions of the thiol with the NC surface in addition to interactions with Cu. In the case of the Cu^{2+} model, the permanent holes in the VB compete for the same CB electron as Cu. When the hole is quickly removed from the NC by thiol, the emission

occurs only through the Cu center. In the case of Cu^+, the BE and Cu emission would be suppressed together.[44]

The Cu emission can only be seen when surface hole traps are present.[19] Higher Cu emission quantum yields can be obtained using a synthesis that results in surface hole traps and no surface electron traps. The intensity of the Cu peak is determined by the efficiency of trapping the hole in the trap states and the intensity of the BE peak is determined by the inefficiency of trapping the electron and the hole in the trap states. The quantum yield of Cu emission is complicated because it increases in the absence of electron traps and presence of hole trap states.[19]

To compare the effect of shell thickness, NCs were grown with different amounts of $CdOA_2$. For thin shell samples, the shell may be too thin for the same thiol-NC interaction to occur (vs. samples prepared with standard Cd amount). With a thinner shell, the NC surface is poorly defined and many defects are present. Addition of thiol has a larger effect on the NC emission. The thiol also may be too close to the Cu and will donate electrons to the VB as well as the Cu so the related emission peaks won't increase. With medium thickness shells, there is more shell material and fewer defects so the NC is less sensitive to the thiol. The Cu emission is high in the original sample (Figure 2.9) because there are more electrons (less holes) present. By adding DDT, electrons are added and the hole traps are removed. Only so many defects exist and once they are removed, the Cu emission will reach its maximum intensity. The thick shell NCs may have a shell that is so thick it is difficult for the DDT to interact with the Cu to donate electrons and remove holes. There are also fewer defects, thus decreasing sensitivity. With a thicker shell, the NC is also larger in size, resulting in a smaller band gap energy. With the smaller band gap energy, the CB lies closer to the Cu state (potentially closer than the thiol), and the Cu captures electrons from the CB and thiol donates electrons to the VB resulting in no BE recombination. The Cu emission has

low intensity in the thick shell sample because there are excess holes competing for the CB electrons that the Cu requires for emission.

After looking at the reduction of the sample, oxidation was studied. Upon oxidizing the sample with air, both peaks decreased in intensity. Oxidizing the sample reduces the amount of electrons in the NC; this means there are less electrons to participate in the BE recombination and the Cu recombination. The peak attributed to the NC was completely quenched upon oxidation. This means that this system is not chemically ratiometrically reversible as anticipated. Dual-emission is only obtained when dopant atoms are present and there is a core/shell structure of different materials.

In summary, when there is less cadmium, the thiol interacts strongly with the VB and Cu of the NC. When more cadmium is present, the thiol interacts weakly with Cu, but can still interact with the VB. When surface traps are present, the PL is dominated by BE emission. Adding thiol removes these traps decreasing the BE emission and increasing the Cu emission, thus creating a ratiometric relationship. When the sample is oxidized, the BE emission is quenched and the Cu emission decreases in intensity. Upon reoxidation, the Cu emission is restored.

Methods

Materials

Zinc stearate ($ZnSt_2$), 1-octadecylamine (ODA, ≥99.0%), trioctylphosphine (TOP, 90%), elemental selenium (Se, ≥99.5%), tri-n-butylphosphine (TBP, 97%), oleic acid (OA, 90%), hexadecylamine (HDA, 90%), copper (II) chloride ($CuCl_2$, 97%), dodecanethiol (DDT, ≥98.0%), tetramethylammonium hydroxide pentahydrate (TMAH, ≥95%), cadmium acetate dihydrate ($CdOAc_2$, 98%), copper acetate ($CuOAc_2$, ≥99.0%), stearic acid, toluene (≥99%), acetone (≥99%), and ethanol (≥99%) were purchased from Sigma Aldrich. Undecylenic acid (Ut_2, 99%) and

1-octadecene (ODE, 90%) were purchased from Acros Organics. Zinc acetate ($ZnAc_2$) and methanol were purchased from Fisher Scientific. Zinc undecylenate ($ZnUt_2$) was purchased from Gelest. All chemicals were used as purchased with no further purification.

Copper Oleate

Copper oleate ($CuOA_2$) was synthesized as described below in a procedure from Klimov and co-workers.[44] TMAH (9 g) and oleic acid (14 mL) were combined in a flask. Methanol was added to dissolve the gel/solid that formed. $CuOAc_2$ (5 g) was dissolved in methanol (400 mL) while heating to ~50 °C. The $CuOAc_2$ solution was added drop wise to TMAH/OA solution overnight. The $CuOAc_2$ solution clogs the separatory funnel periodically and needs to be cleaned out. Once all was combined, the precipitate was filtered, washed with methanol and acetone, and vacuum filtered to dry. Copper oleate was stored at 2 °C.

Cu-doped ZnSe/CdSe

This general procedure was adapted from Klimov, and co-workers.[44] In a 3-neck 100 mL flask, $ZnSt_2$ (63.5 mg) and ODA (0.25 g) were dissolved in ODE (5.0 mL). A condenser was attached to the middle neck, and a septum and temperature probe to each of the side necks. The flask was placed under vacuum for 1 hour at 100 °C. After one hour, the solution was put under nitrogen and the temperature was increased to 270 °C. The Se/TBP mixture (2.4 M, 1 mL) was injected and the solution was immediately cooled to 190 °C. $CuOA_2$ solution (6.3 mg $CuOA_2$ in 1.0 mL ODE) was added drop wise over 3 minutes. After 30 minutes, a solution of $ZnUt_2$ (24.6 mg Ut_2 and 26.3 mg $ZnOAc_2$ in 1.5 g ODE, or 64 mg $ZnUt_2$ in 1.5 g ODE) was added by syringe pump set at a rate of 5 mL/hour. After the hour-long injection was complete, the temperature was increased to 210 °C for 1 hour. A $CdOA_2$ solution (0.2 M) was prepared by dissolving $CdOAc_2$

(73.8 mg) in OA (0.776 mL) and ODE (0.675 mL). The cadmium oleate solution (0.50-1.5 mL) was added to the reaction by syringe pump at a rate of 1 mL/hour. Aliquots were taken at various time intervals. Once shell growth was complete, the heating mantle was removed and the solution was cooled to ~80 °C. The septum was removed, the nitrogen valve closed, and toluene was added. The NCs were divided into 4 test tubes (12 cm x 150 mm), filled approximately half-way with acetone and sonicated to suspend. After centrifugation for 5-10 minutes at 5 kRPM, the NCs formed a pellet at the bottom of the tube (if NCs remained in solution, more acetone was added and they were centrifuged again). The solution was decanted, a pipette full of toluene was added, and the NCs were sonicated to suspend them in toluene. Acetone was added to fill the tubes half way, making sure to mix the acetone and toluene layers, and the tubes are centrifuged again. This process was repeated once more. After the third centrifugation, the liquid was decanted and the NCs were suspended in a small amount of toluene for storage.

Undoped ZnSe/CdSe

The synthesis for ZnSe/CdSe core/shell NCs was the same as the synthesis of Cu:ZnSe/CdSe above without the addition of $CuOA_2$.

Cu-doped ZnSe

The synthesis for ZnSe/CdSe core/shell NCs was the same as the synthesis of Cu:ZnSe/CdSe above without the addition of $CuOA_2$.

Cu-doped ZnSe/ZnSe

The synthesis for Cu:ZnSe NCs was the same as the synthesis for Cu:ZnSe/CdSe above without the addition of a $CdOA_2$ solution.

Chapter 3 - Conclusion and Future Work

Conclusion

It was shown dual-emitting NCs can be synthesized using a growth doping method forming doped core-shell structures. The broad, lower energy red luminescence peak is present when Cu impurities are incorporated into the NC and the green luminescence peak is assigned to band edge emission. To assess the cause of each emission peak, the NCs were synthesized using the same method without adding $CuOA_2$. The resulting NC exhibited only the higher energy emission, suggesting the green luminescence is from band edge, and the broad peak is due to Cu.

To study the importance of the CdSe shell, NCs were made by replacing Cd^{2+} with Zn^{2+}. Without Cd^{2+}, only one emission peak was observed. This showed the Cd^{2+} shell is needed to observe this dual-emission, possibly because the band gap energy of the Cu:ZnSe NCs is outside the Cu energy level. There was also uncertainty of the role of $ZnUt_2$ in the synthesis, including its contribution to the emission. Upon synthesizing NCs without $ZnUt_2$, no significant difference in the absorption or emission were observed. Therefore, the purpose of this step was not readily apparent, although there may be more subtle reasons such as filling of defects in the lattice.

Finally, the redox properties of these samples were studied. The NCs were treated with DDT to reduce them and exposed to air for oxidation. During reduction, the Cu emission increases and the BE emission decreases. To adjust the thiol sensitivity, NCs with different shell thicknesses were synthesized. Thicker shells resulted in lower sensitivity, as expected. Upon drying the sample in air, the intensities of both emission peaks decreased. After this, the Cu emission can be restored with the addition of DDT, but the BE peak was not recovered.

Future work

There are still many aspects of the NCs that need to be studied. To gain a better understanding of the NC PL, time resolved studies should be explored. The redox properties can further be investigated by using different reductants. There were also difficulties with sample-to-sample variations, exacerbated by the multistep synthesis further complicating the system and yielding inconsistent results. Simplification of the synthesis by reducing the number of steps should reduce the sample variations and thus, the disparities in results. In addition, a more simplified system, such as a homogeneous alloy, could give insight into the importance of the Cu position and core/shell structure. Using alternative materials without heavy metals will reduce the toxicity of the NCs, increasing their appeal for applications.

References

(1) Nirmal, M.; Brus, L. *Acc. Chem. Res.* **1999**, 407.
(2) Nozik, A. J.; Beard, M. C.; Luther, J. M.; Law, M.; Ellingson, R. J.; Johnson, J. C. *Chem. Rev.* **2010**, *110* (11), 6873.
(3) Brus, L. *J. Phys. Chem.* **1986**, *90* (12), 2555.
(4) Murray, C. B.; Kagan, C. R.; Bawendi, M. G. *Annu. Rev. Mater. Sci.* **2000**, *30* (1), 545.
(5) Shim, M.; Guyot-Sionnest, P. *Nature* **2000**, *407* (6807), 981.
(6) Colvin, V. L.; Schlamp, M. C.; Alivisatos, A. P. *Nature* **1994**, *370* (6488), 354.
(7) Srivastava, B. B.; Jana, S.; Pradhan, N. *J. Am. Chem. Soc.* **2010**, *133* (4), 1007.
(8) O'Regan, B.; Grätzel, M. *Nature* **1991**, *353* (6346), 737.
(9) Vlaskin, V. A.; Janssen, N.; van Rijssel, J.; Beaulac, R.; Gamelin, D. R. *Nano Lett.* **2010**, *10* (9), 3670.
(10) Tyrakowski, C. M.; Snee, P. T. *Anal. Chem.* **2014**, *86* (5), 2380.
(11) Kamat, P. V. *J. Phys. Chem. Lett.* **2013**, *4* (6), 908.
(12) Pelant, I.; Valenta, J. *Luminescence Spectroscopy of Semiconductors*; Oxford University Press, 2012.
(13) McLaurin, E. J.; Bradshaw, L. R.; Gamelin, D. R. *Chem. Mater.* **2013**, *25* (8), 1283.
(14) Zhang, Z.; Luan, S.; Huang, K.; Zhang, Y.; Shi, Z.; Xie, R.; Yang, W. *J Mater Chem C* **2015**.
(15) Lin, Q.; Makarov, N. S.; Koh, W.; Velizhanin, K. A.; Cirloganu, C. M.; Luo, H.; Klimov, V. I.; Pietryga, J. M. *ACS Nano* **2015**, *9* (1), 539.
(16) trap | solid-state physics http://www.britannica.com/EBchecked/topic/603365/trap (accessed Jan 26, 2015).
(17) Grandhi, G. K.; Viswanatha, R. *J. Phys. Chem. Lett.* **2013**, *4* (3), 409.
(18) Tyagi, P.; Kambhampati, P. *J. Chem. Phys.* **2011**, *134* (9), 094706.
(19) Grandhi, G. K.; Tomar, R.; Viswanatha, R. *ACS Nano* **2012**, *6* (11), 9751.
(20) Green, M. *J. Mater. Chem.* **2010**, *20* (28), 5797.
(21) Kalyuzhny, G.; Murray, R. W. *J. Phys. Chem. B* **2005**, *109* (15), 7012.
(22) Vlaskin, V. A.; Barrows, C. J.; Erickson, C. S.; Gamelin, D. R. *J. Am. Chem. Soc.* **2013**, *135* (38), 14380.
(23) Suzuki, A.; Shionoya, S. *J. Phys. Soc. Jpn.* **1971**, *31* (5), 1455.
(24) Furdyna, J. K. *J. Appl. Phys.* **1988**, *64* (4), R29.
(25) R√?mi Beaulac; StefanT Ochsenbein; DanielR Gamelin. In *Nanocrystal Quantum Dots, Second Edition*; CRC Press, 2010; pp 397–453.
(26) Grandhi, G. K.; Tomar, R.; Viswanatha, R. *ACS Nano* **2012**, *6* (11), 9751.
(27) Norris, D. J.; Yao, N.; Charnock, F. T.; Kennedy, T. A. *Nano Lett.* **2000**, *1* (1), 3.
(28) Pradhan, N.; Peng, X. *J. Am. Chem. Soc.* **2007**, *129* (11), 3339.
(29) Acharya, S.; Sarma, D. D.; Jana, N. R.; Pradhan, N. *J. Phys. Chem. Lett.* **2009**, *1* (2), 485.
(30) Jana, S.; Srivastava, B. B.; Acharya, S.; Santra, P. K.; Jana, N. R.; Sarma, D. D.; Pradhan, N. *Chem. Commun.* **2010**, *46* (16), 2853.
(31) Pradhan, N.; Goorskey, D.; Thessing, J.; Peng, X. *J. Am. Chem. Soc.* **2005**, *127* (50), 17586.
(32) Xie, R.; Peng, X. *J. Am. Chem. Soc.* **2009**, *131* (30), 10645.
(33) Karan, N. S.; Sarma, D. D.; Kadam, R. M.; Pradhan, N. *J. Phys. Chem. Lett.* **2010**, *1* (19), 2863.

(34) Suyver, J. F.; Beek, T. van der; Wuister, S. F.; Kelly, J. J.; Meijerink, A. *Appl. Phys. Lett.* **2001**, *79* (25), 4222.
(35) Bradshaw, L. R.; Knowles, K. E.; McDowall, S.; Gamelin, D. R. *Nano Lett.* **2015**, *15* (2), 1315.
(36) Yang, H.; Holloway, P. H. *Adv. Funct. Mater.* **2004**, *14* (2), 152.
(37) Yang, H.; Holloway, P. H.; Cunningham, G.; Schanze, K. S. *J. Chem. Phys.* **2004**, *121* (20), 10233.
(38) Dabbousi, B. O.; Rodriguez-Viejo, J.; Mikulec, F. V.; Heine, J. R.; Mattoussi, H.; Ober, R.; Jensen, K. F.; Bawendi, M. G. *J. Phys. Chem. B* **1997**, *101* (46), 9463.
(39) Peng, X.; Schlamp, M. C.; Kadavanich, A. V.; Alivisatos, A. P. *J. Am. Chem. Soc.* **1997**, *119* (30), 7019.
(40) Brovelli, S.; Galland, C.; Viswanatha, R.; Klimov, V. I. *Nano Lett.* **2012**, *12* (8), 4372.
(41) Peka, P.; Schulz, H.-J. *Solid State Commun.* **1994**, *89* (3), 225.
(42) Isarov, A. V.; Chrysochoos, J. *Langmuir* **1997**, *13* (12), 3142.
(43) Corrado, C.; Jiang, Y.; Oba, F.; Kozina, M.; Bridges, F.; Zhang, J. Z. *J. Phys. Chem. A* **2009**, *113* (16), 3830.
(44) Viswanatha, R.; Brovelli, S.; Pandey, A.; Crooker, S. A.; Klimov, V. I. *Nano Lett.* **2011**, *11* (11), 4753.
(45) Jawaid, A. M.; Chattopadhyay, S.; Wink, D. J.; Page, L. E.; Snee, P. T. *ACS Nano* **2013**, *7* (4), 3190.
(46) Sarkar, S.; Patra, B. K.; Guria, A. K.; Pradhan, N. *J. Phys. Chem. Lett.* **2013**, *4* (12), 2084.
(47) Pompella, A.; Visvikis, A.; Paolicchi, A.; Tata, V. D.; Casini, A. F. *Biochem. Pharmacol.* **2003**, *66* (8), 1499.
(48) Michalet, X.; Pinaud, F. F.; Bentolila, L. A.; Tsay, J. M.; Doose, S.; Li, J. J.; Sundaresan, G.; Wu, A. M.; Gambhir, S. S.; Weiss, S. *Science* **2005**, *307* (5709), 538.
(49) McLaurin, E. J.; Greytak, A. B.; Bawendi, M. G.; Nocera, D. G. *J. Am. Chem. Soc.* **2009**, *131* (36), 12994.
(50) Lakowicz, J., R. *Principles of Fluorescence Spectroscopy, 3rd Edition*, 3rd ed.; Springer Science.
(51) Snee, P. T.; Somers, R. C.; Nair, G.; Zimmer, J. P.; Bawendi, M. G.; Nocera, D. G. *J. Am. Chem. Soc.* **2006**, *128* (41), 13320.
(52) Khanna, V. K. *Nanosensors: Physical, Chemical, and Biological*; Taylor & Francis, 2011.
(53) Baker, D. R.; Kamat, P. V. *Langmuir* **2010**, *26* (13), 11272.
(54) Jethi, L.; Krause, M. M.; Kambhampati, P. *J. Phys. Chem. Lett.* **2015**, *6* (4), 718.
(55) Varshni, Y. P. *Physica* **1967**, *34* (1), 149.
(56) Peterson, M. D.; Cass, L. C.; Harris, R. D.; Edme, K.; Sung, K.; Weiss, E. A. *Annu. Rev. Phys. Chem.* **2014**, *65* (1), 317.
(57) Vlaskin, V. A.; Beaulac, R.; Gamelin, D. R. *Nano Lett.* **2009**, *9* (12), 4376.
(58) Archer, P. I.; Santangelo, S. A.; Gamelin, D. R. *J. Am. Chem. Soc.* **2007**, *129* (31), 9808.

Appendix A - Uncorrected Spectra

The uncorrected spectra of samples with different shell thicknesses are shown in sample. Figure A.1-Figure A.3.

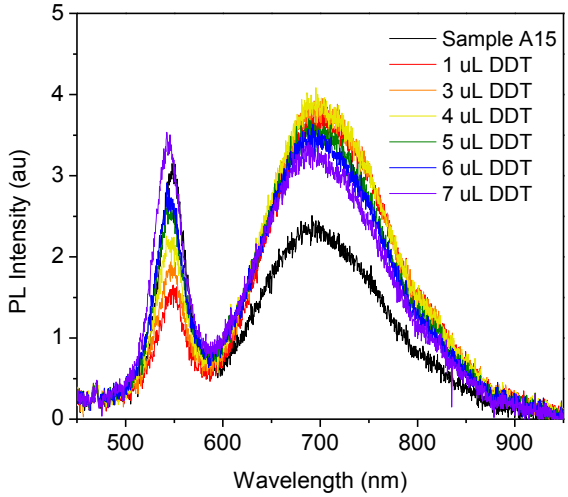

Figure A.1 Uncorrected spectra of thin shell sample.

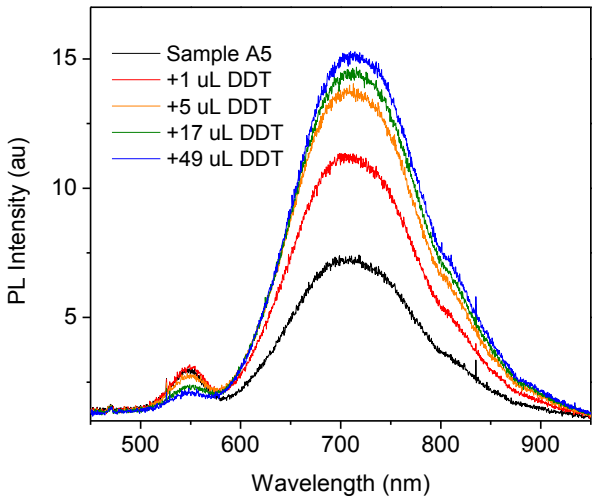

Figure A.2 Uncorrected spectra of medium shell sample.

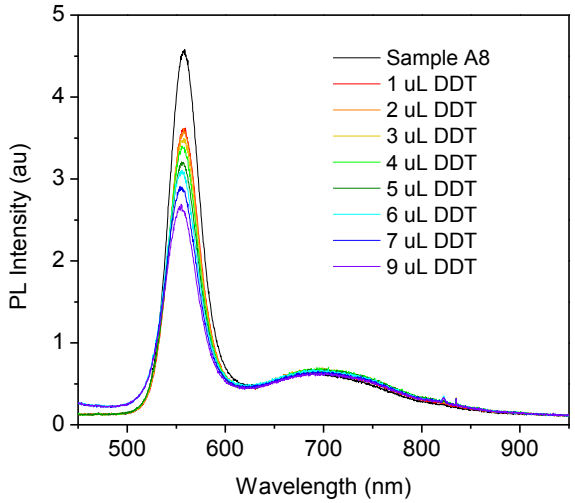

Figure A.3 Uncorrected spectra of thick shell samples.

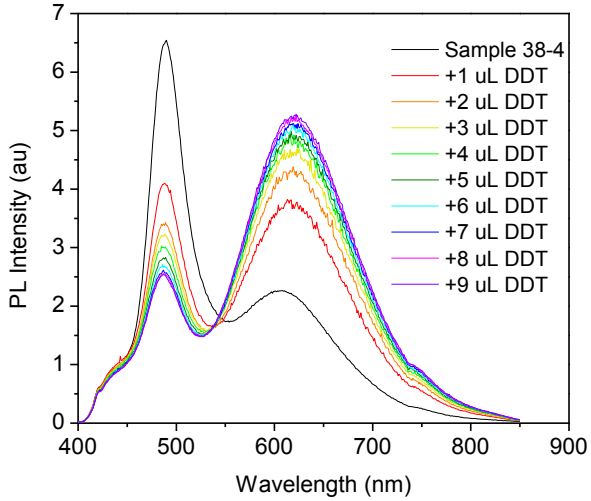

Figure A.4 Uncorrected spectra of Sample 38-4. The corrected spectra is shown in Figure 2.6a and 2.11a.

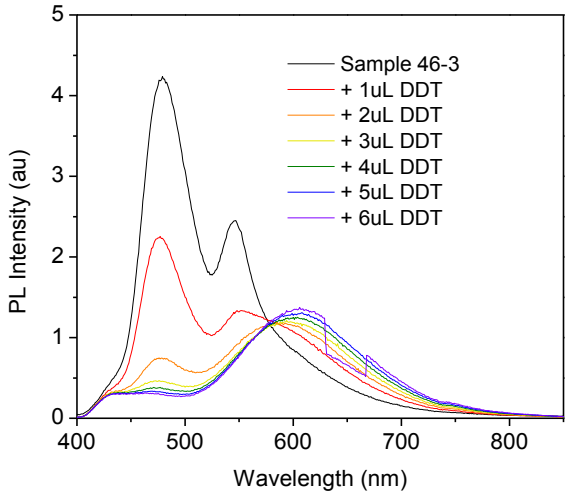

Figure A.5 Uncorrected spectra of Sample 46-3. The corrected spectra is shown in Figure 2.11d.

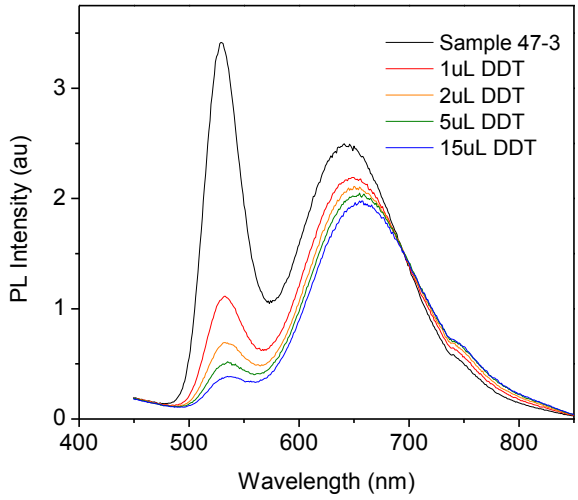

Figure A.6 Uncorrected spectra of Sample 47-3. The corrected spectra is shown in Figure 2.11h.